Fluid detection in carbonate rocks by integrating well logs and seismic attributes

Mohammad Reza Saberi[1]

Abstract

Prestack seismic attributes are efficient tools for hydrocarbon exploration and pore fluid detection with the help of various techniques, such as amplitude variation with offset analysis. Such studies focus mainly on siliciclastics rather than carbonates because detection of fluid effects in carbonate rocks can be masked by their complex pore structure and heterogeneity. Current fluid detection methods from seismic attributes usually rely on a linear background model for P- and S-wave velocities of the water-saturated rocks, and any deviation from this trend is assigned to possible pore fluid changes. This means that the false (or even missed) effect of fluids can be detected in carbonate rocks if inappropriate fluid detection attributes (such as the ones designed for siliciclastics) are used. This is mainly due to the varying pore structure in carbonates, which can make their background model (the model for fully water-saturated rock) mainly nonlinear. I observed that this nonlinearity in the carbonates background model becomes more linear by using P-velocity squared versus the product of the P- and S-velocities crossplot instead of P-velocity versus S-velocity crossplot. Furthermore, I used this proposed crossplot to define a more appropriate background model for my carbonate sequence containing some percentages of gas. I derived a new seismic fluid attribute based on the proposed background model, and I compared the results with various other fluid factors. My results highlight fluid changes more brightly and consistently than existing alternatives for carbonate environments.

Introduction

Seismic reflection amplitudes reveal information about the fluid content of the rocks constituting seismic reflectors. Hydrocarbon reservoirs may, therefore, be detected from seismic amplitude anomalies using attributes such as the fluid factor equation (Smith and Gidlow, 1987). On the stacked seismic data, identifications of bright spots, dim outs, phase reversals, or flat spots are also interpreted as direct hydrocarbon indicators. However, such hydrocarbon-related amplitude anomalies are not the only amplitude anomalies that could be caused by reservoir rock property changes, especially for carbonate rocks. The relationships between reservoir and seismic properties are more complex for carbonate rocks than they are for siliciclastics due to their highly variable pore structures (Wang, 1997; Anselmetti and Eberli, 1999). This can be observed on their porosity-velocity crossplots with a high scattering pattern and as a nonlinear trend on their V_P and V_S relationship. This is the result of the coexistence of various pore types with different stiffness in carbonates in such a way that increasing the volume fraction of soft pores (e.g., cracks) can make them more sensitive to the pore fluid properties (Saberi, 2010). Thus, to reduce such nonuniqueness in reservoir property interpretation (especially for carbonate rocks), prestack techniques such as amplitude variation with offset (AVO) need to be analyzed and modeled using rock-physics techniques. Rock physics is an efficient tool for investigating rock microstructure effects on seismic properties and can help with resolving the nonuniqueness problem in reservoir property interpretation.

This paper investigates the fluid factor equation (Smith and Gidlow, 1987) in more detail, and it proposes a modification to it that is applicable for detecting fluid anomalies within carbonate layers. Its applicability will then be tested on a carbonate data set consisting of two exploration wells (A and B) and a connecting 2D seismic line with near-, far-, and full-offset stacks. The carbonate interval has been characterized in terms of depositional evolution, style of diagenesis, and porosity development into four stages: mixed siliciclastic and carbonate, shallow water, open marine, and deep/cold water. Furthermore, these depositional evolution stages are classified into nine different lithologic units based on the biota and 12 associated microfacies (Ehrenberg et al., 1998a, 1998b). The proposed modification adopts the existing fluid factor equation for carbonates by using a more linear behavior on $V_P^2 - V_P V_S$ crossplot as the background model. This, in turn, brightens up the

[1]CGG, GeoSoftware, The Hague, Netherlands. E-mail: reza.saberi@cgg.com.

Manuscript received by the Editor 12 April 2019; revised manuscript received 15 July 2019; published ahead of production 16 September 2019; published online 08 November 2019. This paper appears in *Interpretation*, Vol. 8, No. 1 (February 2020); p. SA1–SA10, 7 FIGS., 2 TABLES.
http://dx.doi.org/10.1190/INT-2019-0054.1.

seismic fluid anomaly with more continuous effects on the seismic section.

Background and methodology

In general, AVO analysis aims to extract information about lithologic conditions and pore fluid properties from reflection amplitudes and their variation with offset. The AVO assumption is that the reflection coefficient from a plane boundary separating media of different acoustic impedances is also a function of the incidence angle, which is normally expressed through the nonlinear Zoeppritz (1919) equations. Linear approximations of Zoeppritz equations (e.g., Koefoed, 1962; Aki and Richards, 1980; Wiggins et al., 1983) are easier to analyze and more applicable for AVO analysis. Aki and Richards (1980) present a simplified version of the Zoeppritz equations relevant for precritical reflections. Wiggins et al. (1983) and Shuey (1985) use the Aki and Richards (1980) results to show that when considering a small impedance contrast between reflection and refraction waves, and $V_P \approx 2V_S$, a linearized version of the reflection coefficient R_{pp} can be written as

$$R_{pp}(\theta) \approx R_P + G \sin^2 \theta, \tag{1}$$

where θ denotes the incidence angle, G is the AVO gradient, and R_P is the AVO intercept or normal incidence P-wave reflection coefficient and can be approximated by

$$R_P = \frac{1}{2}\left(\frac{\Delta V_P}{V_P} + \frac{\Delta \rho}{\rho}\right), \tag{2}$$

where $\Delta\rho = \rho_2 - \rho_1$, $\rho = 1/2(\rho_1 + \rho_2)$, $\Delta V_P = V_{P_2} - V_{P_1}$, and $V_P = 1/2(V_{P_1} + V_{P_2})$. Here, V_P denotes the P-wave velocity, ρ is the density, and the subscripts 1 and 2 refer to the medium properties of our two-layer model (reflection and refraction media). The AVO gradient (G) is shown (Wiggins et al., 1983) to be related to the normal incidence P- and S-wave reflectivities, R_P and R_S, by

$$G = R_P - 2R_S, \tag{3}$$

with

$$R_S = \frac{1}{2}\left(\frac{\Delta V_S}{V_S} + \frac{\Delta \rho}{\rho}\right), \tag{4}$$

where ΔV_S and V_S are defined similarly to the ΔV_P and V_P definition for R_P.

Ostrander (1984) is among the first to show that gas-saturated sandstones have lower Poisson's ratios (and V_P/V_S ratios) than water-saturated sandstones. This means that AVO techniques can be potentially used to detect gas-bearing sandstones from surface seismic data alone. Later, Smith and Gidlow (1987) develop a pore fluid indicator using a combination of G, R_P, and R_S, referred to as fluid factor (ΔF). Furthermore, Goodway et al. (1997) show the use of Lamé's elastic parameters (λ and μ) and their products with density ρ, as useful attributes for fluid and lithology discrimination. The term μ is the shear modulus, and λ is defined as

$$\lambda = K - \frac{2}{3}\mu, \tag{5}$$

where K is the incompressibility. In particular, λ and $\lambda\rho$ were deduced as potential direct hydrocarbon indicators. As an alternative to the use of R_P, R_S, and G, Connolly (1999) formulates the concept of elastic impedance. When combined with acoustic impedance, elastic impedance may be applied to separate gas sands from wet sands and shales. The elastic impedance is a generalization of the acoustic impedance for variable incidence angles, and it is an appropriate AVO parameter to be used in seismic inversion (Cambois, 2000). However, to further quantify the effect of lithologic conditions or their pore fluid content from reflectivity data, rock-physics relations have to be embedded within seismic attributes. Castagna et al. (1985) establish a linear empirical relationship between V_P and V_S for water-saturated siliciclastic rocks (sandstones and shales), which, when considering velocities in ms^{-1}, is given by

$$V_P = 1.16V_S + 1360. \tag{6}$$

Neglecting the density effects on R_P and R_S (i.e., $\Delta\rho = 0$) and differentiating equation 6 with respect to V_S yields a relation between $R_P = (\Delta V_P/2V_P)$ and $R_S = (\Delta V_S/2V_S)$ for water-saturated siliciclastic rocks as

$$R_P = 1.16\left(\frac{V_S}{V_P}\right)R_S. \tag{7}$$

Thus, for reflections between water-saturated rocks (i.e., shale/sand), the fluid factor ΔF vanishes. Then, ΔF (Smith and Gidlow, 1987) is defined as

$$\Delta F = R_P - \alpha R_S, \tag{8}$$

where $\alpha = 1.16V_S/V_P$. Whenever $|\Delta F| > 0$, this should indicate a shale/sand reflection boundary in which one of the layers is not fully water saturated. Deriving V_S/V_P for real data implies that the P-wave interval velocities of the two layers must be estimated, for example, from stacking velocities. Subsequently, the corresponding interval S-wave velocities can be found using the empirical V_P-V_S relationship, e.g., in this case the mudrock line. Fatti et al. (1994) formulate this for studying time-varying amplitudes by defining the fluid factor as

$$\Delta F(t) = R_P(t) - \beta(t)R_S(t), \tag{9}$$

where $\Delta F(t)$ is the fluid factor extracted for each time sample of the normal moveout-corrected seismic gather and $\beta(t)$ is a slowly time-varying gain function that should be extracted locally, and it varies slightly from area to area with depth. The term $\beta(t)$ slightly changes within a reservoir and can be considered as a constant value based on the given surrounding water-saturated

sediments. Furthermore, Smith and Sutherland (1996) propose a quality factor to find the optimum $\beta(t)$ by defining it as

$$\beta(t) = a\frac{V_S(t)}{V_P(t)}, \tag{10}$$

where a is the slope of the linear relationship between V_P and V_S for the water-bearing zones, $V_P(t)$ is determined from stacking velocities, and the corresponding $V_S(t)$ is defined from an empirical relationship between V_P and V_S. This infers that reflections from water-saturated sediments that do not follow the mudrock line (such as carbonate rocks) could be wrongly brightened up using equations 8 and 9 (Avseth et al., 2005). Furthermore, this means that using these attributes can create false fluid anomalies for the interbedded carbonate layers within a clastic sedimentary column. However, studies by Rafavich et al. (1984) and Li and Downton (2000) show significant effects of gas on the AVO behavior in carbonate rocks, which again indicates the applicability of AVO for detecting fluid anomalies within carbonate sequences if proper fluid attributes are designed. This study aims to design a seismic attribute to detect fluid effects in carbonates. This attribute will be tested, furthermore, on a carbonate data set for validation, and the results will be compared with the common fluid attributes.

Fluid detection attribute for carbonates

This paper seeks to obtain a simple approach to define background trends used for fluid detection in carbonate rocks similar to the one found for siliciclastics by Smith and Gidlow (1987). Figure 1a shows V_P versus V_S for a set of modeled data, in which the mineral and fluid (brine) properties are constant and the pore structure and porosity varied. The modeling was performed using a differential effective medium approach (Berge et al., 1992) with inclusions defined by the pore aspect ratio and their volume fractions from the total porosity (ranges between 0% and 20%). Details of the parameters used in the modeling are provided in Tables 1 and 2. In Table 2, P_1 to P_4 represent different defined scenarios for pore geometry based on different aspect ratios; P_1 represents the stiffest pore geometry by having all pores

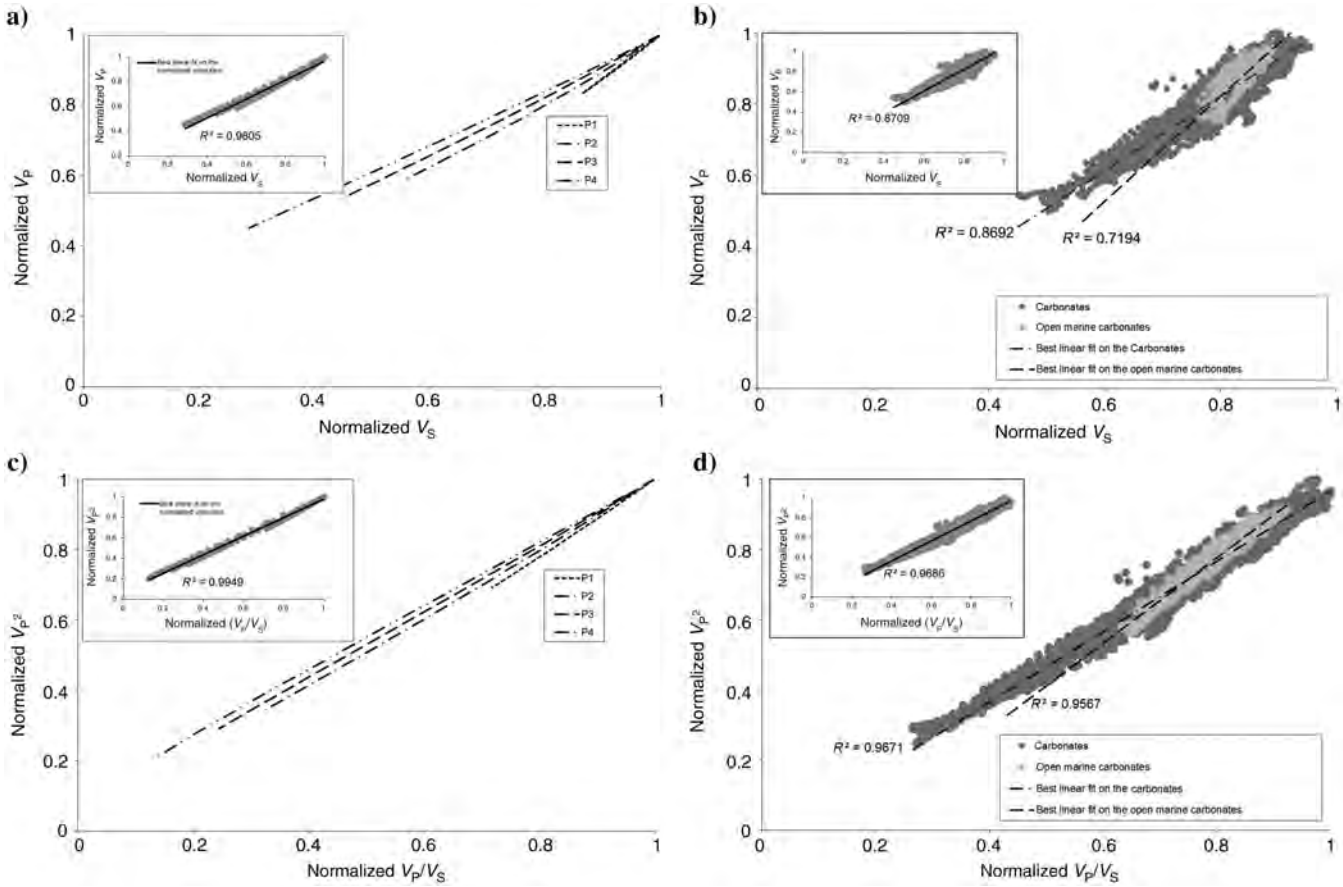

Figure 1. (a) Normalized and modeled V_P versus V_S crossplots for a brine-saturated limestone with different pore aspect ratios and their volume fractions (P_1 to P_4 as given in Table 2) and (b) the same crossplot as (a) given for the well logs of well A. This well is penetrating within the carbonate sequence consisting of different depositional environments and reveals a prominent change in water saturation within the open marine sediments. (c and d) The normalized V_P^2 versus V_PV_S crossplots of data are shown in (a and b). It is clear that classifying carbonates based on the pore structure along with using a V_P^2 versus V_PV_S crossplot can help with a more linear background response.

with aspect ratios equal to one. Then, gradually volume fractions of lower aspect ratios are increased and as a result pore geometry becomes softer (from P_2 to P_4). Figure 1b shows V_P versus V_S for two carbonate sequences obtained from the well log used in this study. Figure 1a and 1b clearly demonstrates that there is not a linear trend between the two velocities. In both plots, a line has been fitted to the data points. However, if we plot them in a V_P^2 versus $V_P V_S$ crossplot, then we can obtain a more linear trend (Figure 1c and 1d). This is confirmed by the correlation coefficients of the lines fitted to the crossplots in the given figures. Therefore, a linear relationship between V_P^2 versus $V_P V_s$ can be considered as the background trend instead of the mudrock line to derive a new fluid factor for carbonates. This relationship, in general, can be written as

$$V_P^2 = a' V_P V_S + b', \tag{11}$$

where a' and b' are the regression coefficients. Differentiation of equation 11 with respect to V_S gives

$$2V_P \frac{\Delta V_P}{\Delta V_S} = a' \left(V_S \frac{\Delta V_P}{\Delta V_S} + V_P \right). \tag{12}$$

Hence, we obtain

$$\frac{V_P}{V_S} R_P = \frac{a'}{2} (R_P + R_S) \tag{13}$$

considering equations 2 and 4 and neglecting the density effects ($\Delta\rho$) on R_P and R_S. Therefore, a seismic fluid factor for carbonate can accordingly be defined as

$$\Delta F = R_P - \gamma R_S, \tag{14}$$

where γ is a parameter given as

$$\gamma = \frac{1}{\frac{2}{a'} \frac{V_P}{V_S} - 1}. \tag{15}$$

This equation has the same format as previous fluid factor equations but with a different coefficient for R_S. This coefficient needs to be defined using well-log data from crossplot analysis considering the related depositional environment. To test this modified fluid factor, a reflection within a simple two-layer model is assumed. The layer properties were obtained from the modeling results of Figure 1, and the parameters and details of the model are given in Tables 1 and 2. Figure 2 shows derived fluid factors considering various porosities of the refraction (reservoir) medium, based on equation 8 (Smith and Gidlow, 1987), and the modified fluid factor given in equation 14. For the application of equation 8, the mudrock line ($a = 1.16$) and a locally calibrated V_P versus V_S slope ($a = 1.49$) were used. For the modified fluid factor, the slope was defined according to the results of Figure 1c ($a' = 0.9$). The modified fluid factor is

Table 1. The elastic constants used in the present model for calcite, brine, and light gas.

Mineral and fluid	Density (g/cm^3)	Bulk modulus (GPa)	Shear modulus (GPa)
Calcite	2.71	76.8	32
Brine	1.05	2.2	0
Light gas	0.07	0.0177	0

Table 2. The assumed pore models. The term α is the pore aspect ratio, and P_1–P_4 are their corresponding volume fractions.

α	P_1	P_2	P_3	P_4
1	1	0.65	0.60	0.45
0.1	0	0.20	0.20	0.20
0.01	0	0.13	0.13	0.20
0.001	0	0.20	0.07	0.15

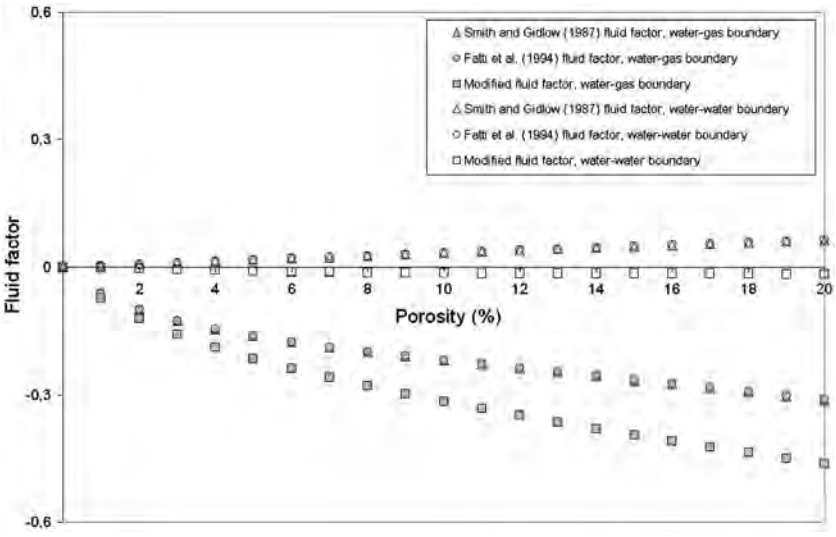

Figure 2. The calculated fluid factors for a two-layer carbonate model (limestones) in which layer 1 is water filled and layer 2 is water or gas filled. The pore aspect ratio for layer 1 is defined from P_2 (Table 2), and the pore aspect ratio for layer 2 is defined from P_4 (Table 2). The porosities of both layers vary between 0% and 20%, and different fluid factors are calculated accordingly. This figure investigates the fluid factor response for two scenarios: (1) Both layers are water saturated (the open symbols) and (2) layer 1 (upper layer) is water saturated, whereas layer 2 (under layer) is gas saturated (the gray-filled symbols).

seen to give the strongest response of the three. As a reference, the various fluid factors are also displayed in the case of a water-water reflection, which theoretically should give zero response.

Application of the derived equation on a carbonate sequence

The proposed fluid attribute, along with other attributes, was applied to the carbonate data set. Figure 3 shows well logs for the two wells highlighting the gas-saturated limestone within the open marine heterozoan limestone (the black circles). The open marine depositional environment (with possibly a different pore geometry compared with the other depositional environments) is partially saturated with gas, whereas the other carbonate depositional environments are fully brine saturated. Furthermore, AVO parameters are calculated for both wells using blocked elastic logs. It can be seen that gas will, relative to full water saturation, decrease V_P/V_S and K/μ, whereas the gradient parameter G becomes positive at the bottom of the gas-saturated zone (Figure 4).

To analyze the rock properties of the carbonate sequence compared with the siliciclastics and open marine limestone, the V_P-V_S crossplot for these two wells is compared in Figure 5. It can be seen that the carbonate line deviates from the mudrock line (siliciclastics) by a higher slope. In addition, two different V_P versus V_S trends can be observed within the carbonate interval in which the open marine heterozoan limestone deviates with a higher slope from the entire carbonate sequence. This deviation can be attributed to their fluid content as well as their heterogeneous pore geometry caused by variations in their depositional environment (Anselmetti and Eberli, 2001). Figure 6 displays the same well logs on the V_P^2 versus V_PV_S crossplots in which a better linear relationship and improved fit is observed. This improvement in linearity as illustrated in Figure 2 can be related mainly to the reduction in pore geometry effects on the scattered and nonlinear behavior in the V_P versus V_S crossplot. This means that the deviation between the open marine limestone and the entire carbonate sequence should now mainly be related to their fluid content.

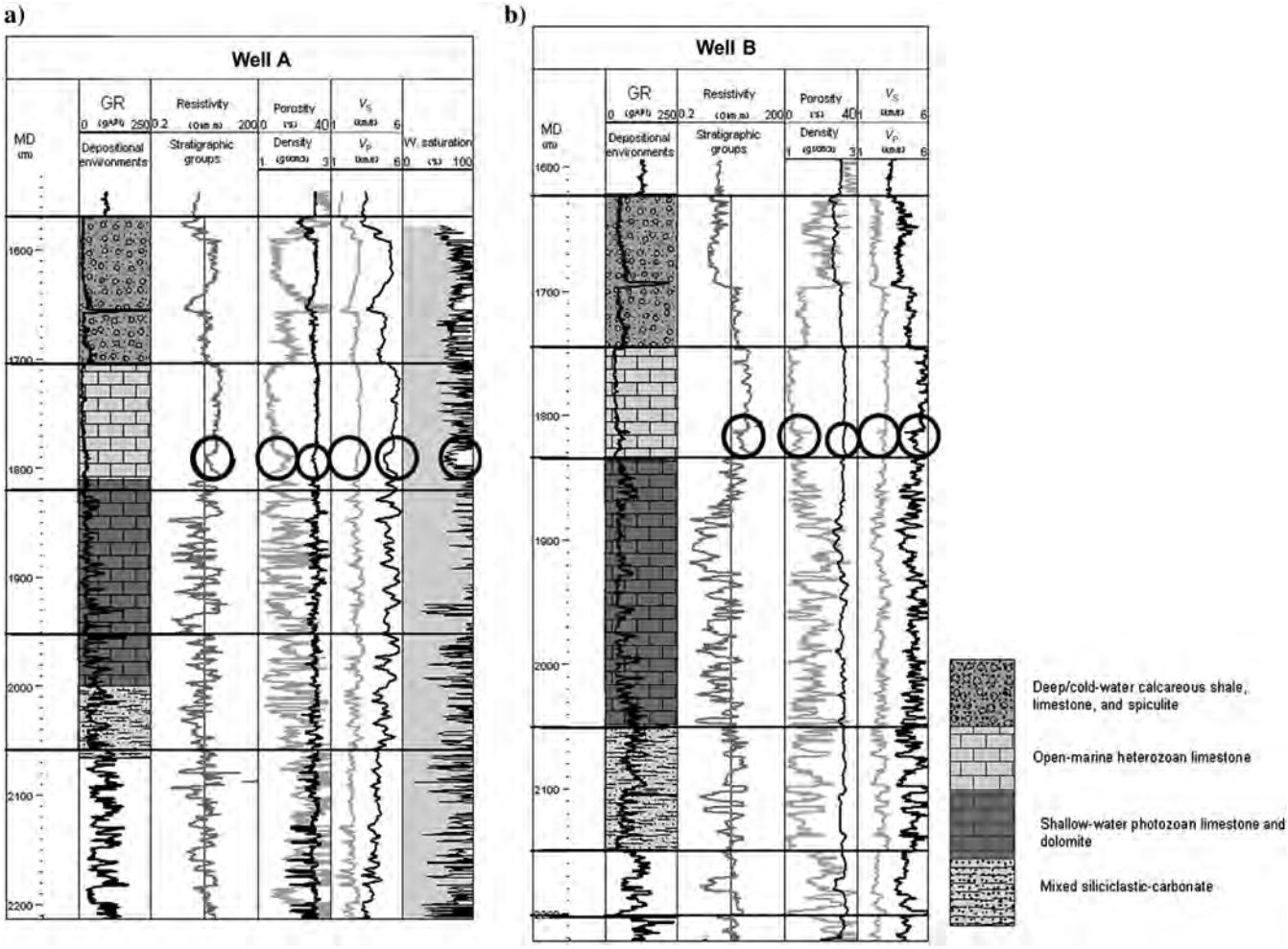

Figure 3. Well-log data including the gamma ray, porosity, density, resistivity, saturation, and sonic velocities (P- and S-wave) for wells A and B (Saberi, 2010). A water saturation log (the first track from the right in a) was only available from well A. The same behavior of the gas-saturated interval on well A logs (resistivity, porosity, density, V_P, and V_S) can also be detected on the same logs for well B (the black circles), which is a good indicator of the existence of gas in that interval for well B.

In the following, the well data (Figures 5 and 6) are used to determine the coefficients α, β, and γ of the various fluid factors using relevant equations set out in the previous section. Here, the V_S/V_P ratios are obtained from the blocked P-velocities above and below the reflection boundary, with the corresponding S-velocities predicted using the relevant background V_P-V_S model. Then, fluid attributes are calculated using four different models:

1) The Smith and Gidlow (1987) fluid factor (equation 8):

$$\Delta F_1 = R_P - 0.74R_S. \tag{16}$$

Here, α (0.74) is calculated based on the mudrock line as shown in Figure 5a and 5b (the black dots).

2) The Fatti et al. (1994) fluid factor (equation 9) using the carbonate sequence as the background model:

$$\Delta F_2 = R_P - 0.98R_S. \tag{17}$$

Here, β (0.98) is calculated based on the best fit line on the entire carbonate sequence as shown in Figure 5a and 5b (the gray dots).

3) The Fatti et al. (1994) fluid factor (equation 9) using only the open marine depositional environment (a member of the carbonate sequence) as the background model:

$$\Delta F_3 = R_P - 1.14R_S. \tag{18}$$

Here, β (1.14) is calculated based on the best fit line on the open marine carbonate sequence as shown in Figure 5c and 5d (the light-gray dots).

4) The proposed approach of using the linear behavior of V_P^2 versus V_PV_S crossplots (equation 14)

$$\Delta F_4 = R_P - 0.37R_S. \tag{19}$$

Here, γ (0.37) is calculated based on the best fit line on the entire carbonate sequence as shown in Figure 6a and 6b (the gray dots).

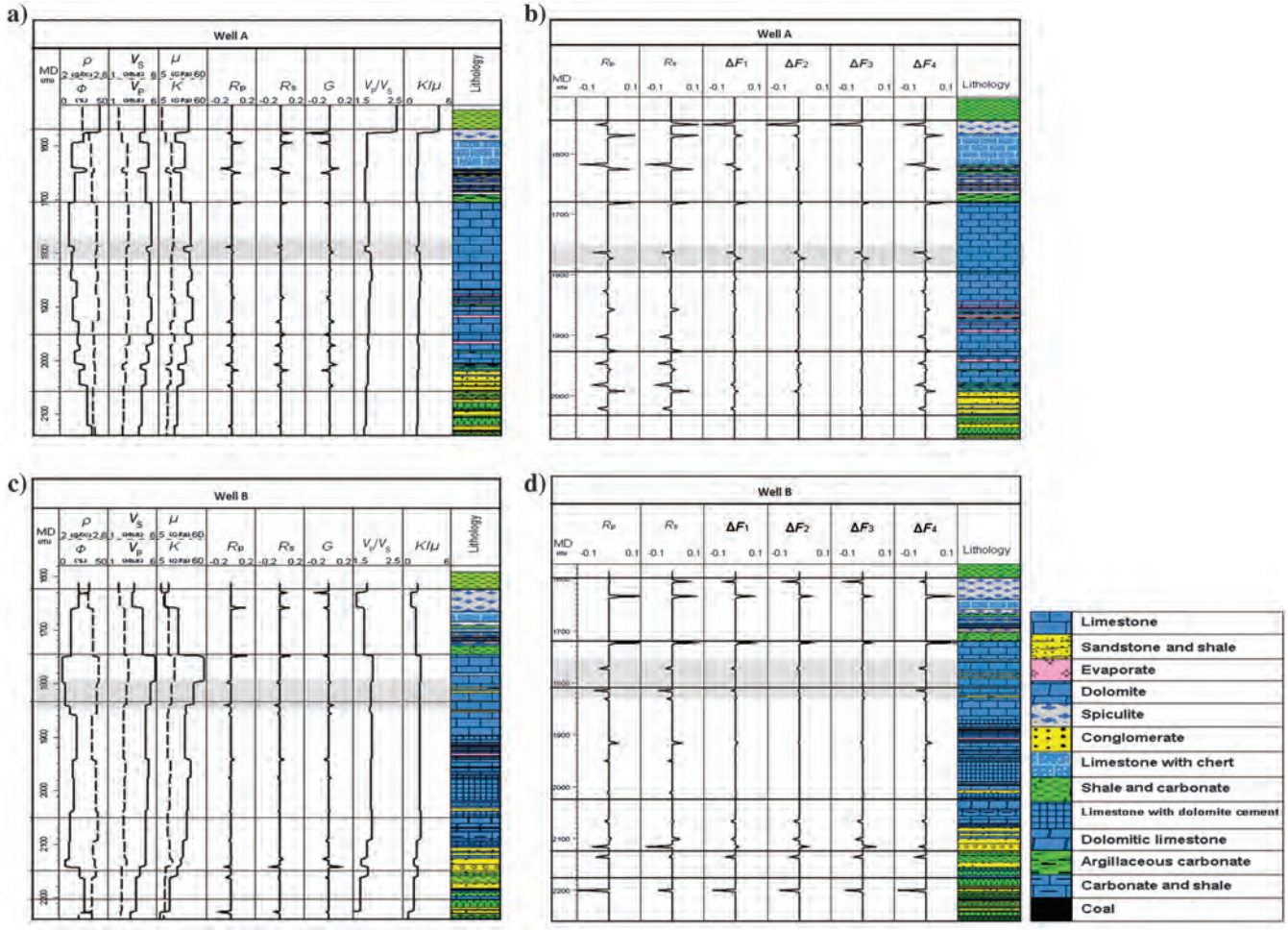

Figure 4. (a and c) The AVO parameters (R_P, R_S, and G) and (b and d) various fluid factors (ΔF_1- ΔF_4) at well locations calculated using well data. Also shown are the P-velocity V_P, S-velocity V_S, porosity Φ, bulk modulus K, and shear modulus μ, V_P/V_S, and K/μ. The gray box shows the assumed zone for saturation changes within the limestone interval. The newly introduced fluid attribute (ΔF_4) is seen to be more brightened within this interval compared with the other fluid attributes (adopted from Saberi, 2010).

Figure 4b and 4d shows the results of these four fluid factor equations on logs from well A and well B. Furthermore, R_P and G are derived from the near- and far-stack seismic data and accordingly the same fluid attributes (ΔF_1, ΔF_2, ΔF_3, and ΔF_4) are calculated for the 2D seismic line connecting these two wells. The results are presented in Figure 7 in which four different fluid sections are compared.

Results and discussion

Figure 4b and 4d shows the various fluid attribute logs (ΔF_1, ΔF_2, ΔF_3, and ΔF_4) using the refined well data (Figure 4a and 4c) in which the gray band highlights the depth section of the assumed partly gas-saturated layer. All of the four calculated fluid attribute logs (Figure 4b and 4d) consistently brighten up the fluid-containing reflector, but the proposed fluid attribute (ΔF_4) clearly gives the strongest response. These various fluid attributes are applied to the available seismic section (Figure 7) to generate four different fluid attribute sections. As these sections are scaled in the same way, the amplitudes are directly comparable. Within the carbonate sequence, indicated by the white background, the modified fluid factor ΔF_4 appears less noisy, and it also displays the interface as more continuous, particularly in the rightmost part of the section. Note that γ coefficient for calculating ΔF_4 is calculated using the entire carbonate sequence (Figure 6a and 6b), and the open marine depositional environment (the gas-bearing interval) deviates from this general trend (Figure 6c and 6d). This deviation is attributed mainly to different fluid content using ΔF_4 as the variation in lithology is seen to be gentle based on the R_S section. Here, some of the events above and below this interface also appear to be brighter and more continuous compared with the other sections. However, within the siliciclastic sequence below, ΔF_4 indicates false fluid anomalies that are not shown by ΔF_1-ΔF_3. This is as expected because the introduced

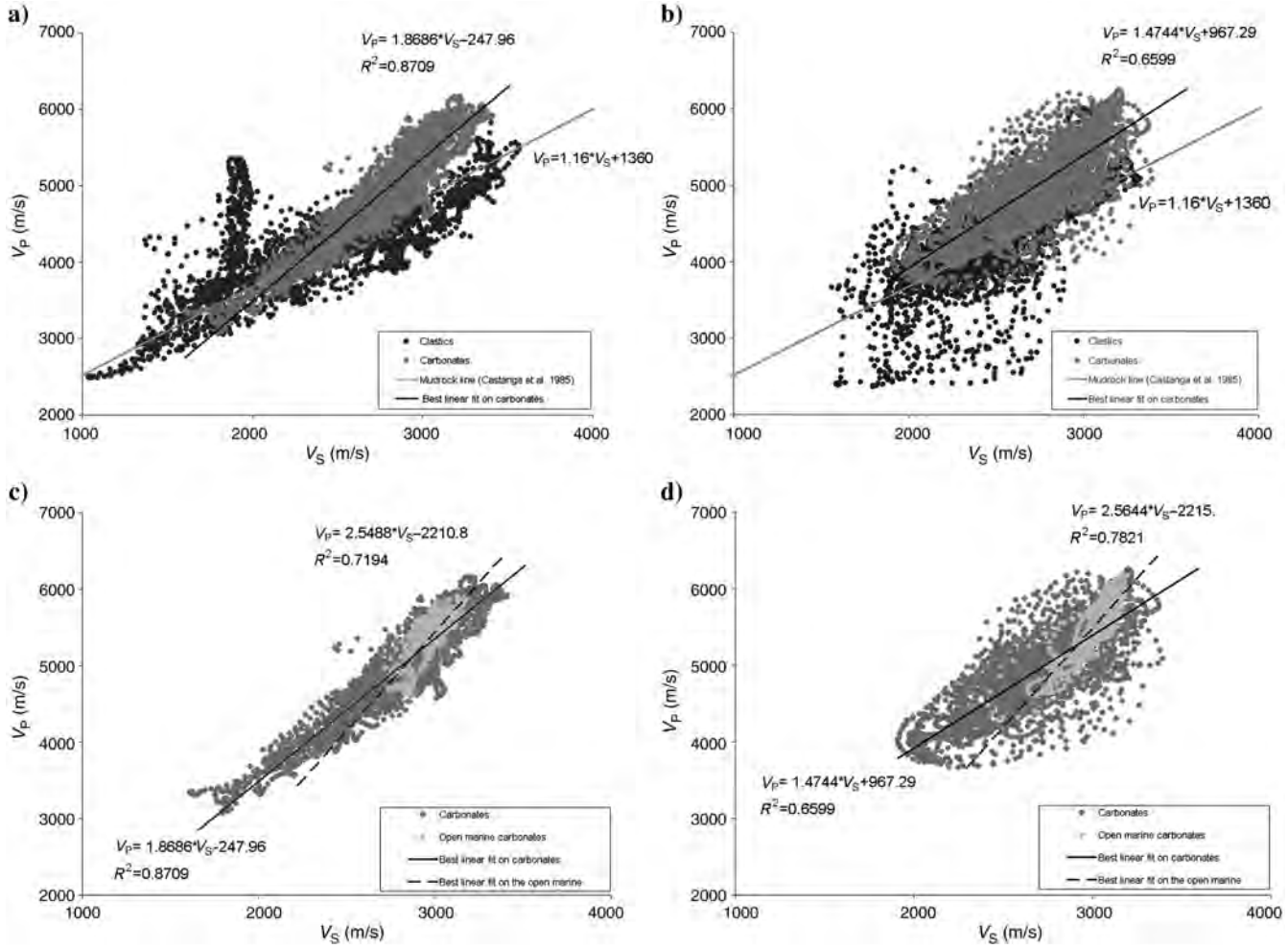

Figure 5. Crossplots of V_P versus V_S from well-log data for clastics (the mudrock line shown in the black dots) and carbonate (the gray dots) interval for (a) well A and (b) well B. The open marine carbonates (the light-gray dots) are furthermore shown within the carbonate interval (the gray dots) in (c) well A and (d) well B. (a and b) How carbonate intervals deviate from the clastic trend (mudrock line). Furthermore, (c and d) show how even different depositional environments (open marine in this case) within the carbonate interval can deviate from the general carbonate trend. The inserted lines are the best fit to the well data, and R^2 is their coefficient of determination.

modification is specifically designed for reflections within carbonate rocks. This example particularly demonstrates the need to establish the main lithologic units, before interpreting fluid anomalies.

The strong fluid response for all fluid factors can be understood from Figures 2 and 4 because the porosity of the considered zone is moderate resulting in a value of the same range for all fluid factors. The term ΔF_4 should further outperform the others by looking for a linear background trend in which the pore geometry effects are minimized. This carbonate attribute is designed based on the Smith and Gidlow (1987) approach for siliciclastics using P- and S-wave reflectivity information along with a more appropriate background model. The estimation of R_P and G is based on the assumptions of weak layer contrasts, a relatively small interval of precritical incidence angles, and on the $V_P \approx 2V_S$ relation. Thus, this new approach may suffer from the weaknesses inferred by these assumptions. In general, V_P for carbonates is usually greater than for siliciclastics, which makes this latter assumption better for carbonates than for siliciclastics. In the derivation, the density effects on the reflection coefficients (e.g., R_P and R_S) are ignored. This assumption may be more adequate to consider for reflections within carbonate layers rather than within siliciclastic rocks because the mineralogy of carbonates is more uniform. In fact, carbonates of the same porosity but different pore structure may give strong differences in their P- and S-velocities, whereas their densities are equivalent. The basic concept of the new fluid attribute is to impose a linear correlation between the P-velocity squared versus the product of P- and S-velocities. This assumption holds for our data, but it should be further evaluated for other carbonate velocity measurements.

Seismic attributes such as the fluid factor are important tools to consider in the screening phase of seismic exploration because they pinpoint areas in which more sophisticated methods should be directed. For evaluation of prospects in siliciclastic systems, qualitative seismic interpretation tools based on AVO data, alternatively on acoustic and elastic impedances, and rock-physics templates, have been developed (Avseth et al., 2005). However, the commonly used rock physics

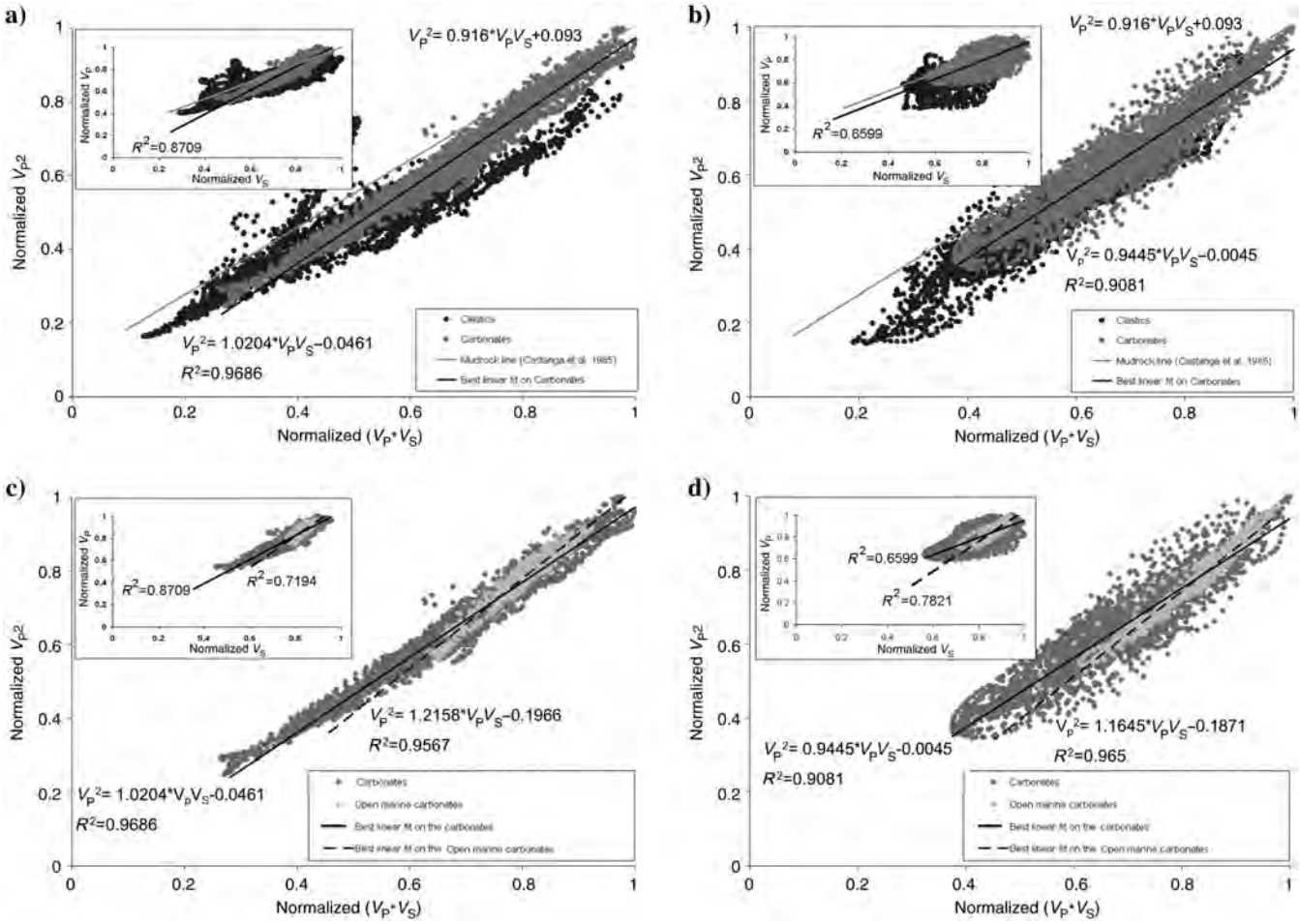

Figure 6. Crossplot of normalized V_P^2 versus $V_P V_S$ with the same log data as in Figure 5. Normalized V_P versus V_S crossplots are inserted for better comparison. The correlation coefficients show that V_P^2-$V_P V_S$ for carbonates is better linearized compared with V_P versus V_S. Note that the mudrock line in (a and b) is calculated by deriving V_S from V_P using the mudrock line and then computing their combination as V_P^2 and $V_P V_S$ and normalizing them.

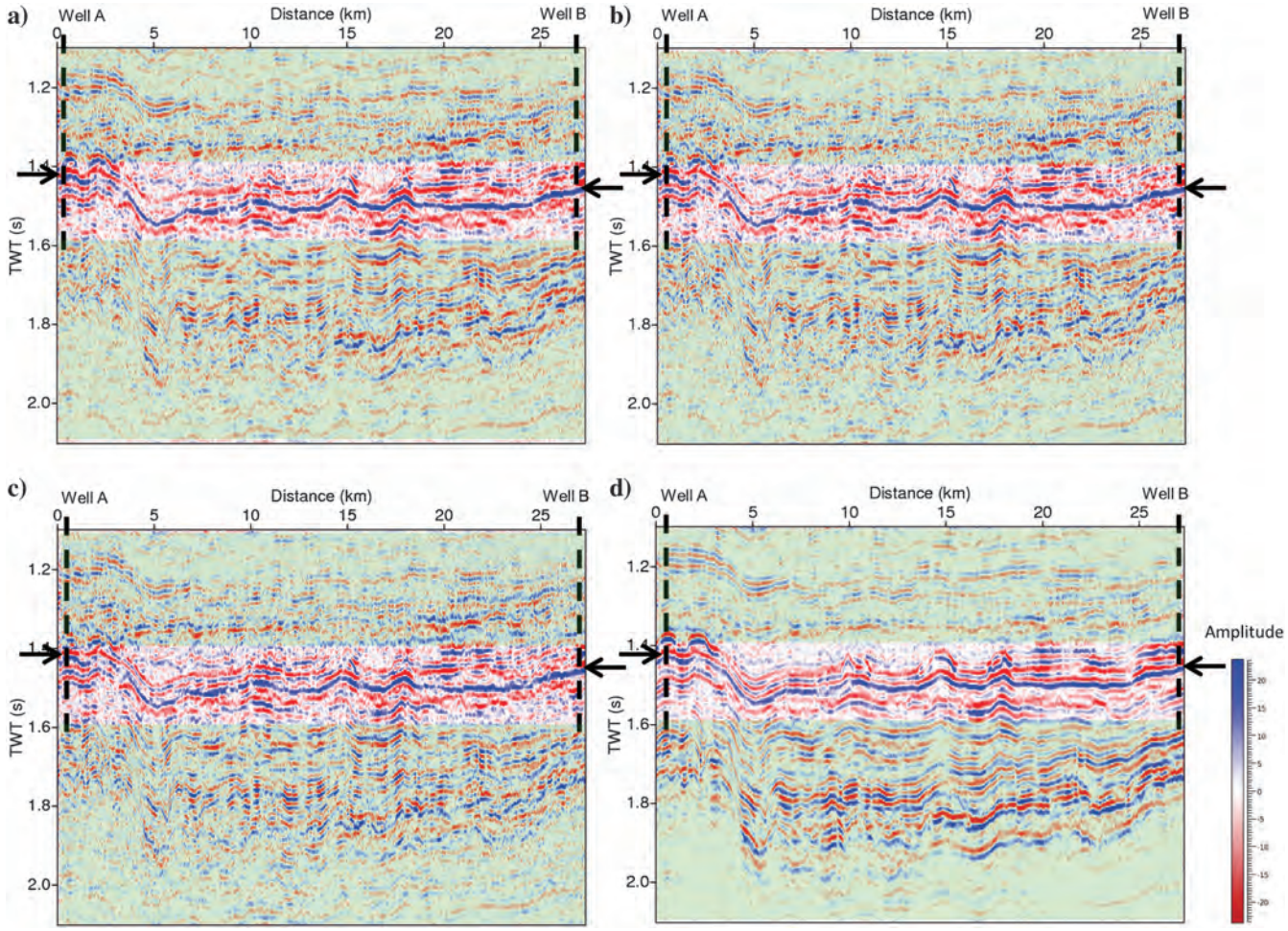

Figure 7. Various fluid factor sections obtained using near- and far-stack data: (a) $\Delta F1$, (b) $\Delta F2$, (c) $\Delta F3$, and (d) $\Delta F4$. The dashed lines show the well positions, and the black arrows indicate the top of the partially gas-saturated carbonate layer (adopted from Saberi, 2010). These four sections are derived using four different fluid factor equations. It can be seen that all of them highlight fluids effect through the section, but the proposed (d) fluid factor clearly gives the strongest and most continuous response.

templates do not take into account the strong impact of the pore structure, which is decisive for the seismic response of carbonates. Thus, reevaluating commonly used seismic attributes in siliciclastics for the complex pore geometry of carbonates is a necessary step in their seismic characterization.

Conclusion

Detection of pore fluid anomalies in subsurface rocks from seismic data is essential in exploration for hydrocarbons. Tools developed for siliciclastic rocks may not work properly when they are applied to reveal reservoir and fluid conditions from seismic data for carbonate rocks. The main reason is related to their highly varying pore geometry, which makes their fluid signature within seismic data more complex to understand. Often-used seismic attributes for fluid detection are based on a linear relationship between P- and S-velocities, which is not an adequate assumption for carbonates.

In this study, a linear relationship between the P-velocity squared and the product of the P- and S-wave velocities was proposed as the background model for designing a seismic pore fluid attribute in carbonates. The background model could be estimated from P- and S-wave velocity data obtained from well logs, or alternatively, from rock-physics modeling. The proposed fluid attribute was demonstrated to work for reflections within a carbonate sequence, in which a fully water-saturated layer overlays a partly gas-saturated layer. This study also highlighted the necessity of doing lithology prediction, before fluid prediction, as a pore fluid indicator designed for siliciclastics can produce false fluid anomalies in carbonates, and vice versa.

Data and materials availability

This paper was part of my Ph.D. thesis published in 2010 and the data are the same as in my Ph.D. thesis.

References

Aki, K., and P. G. Richards, 1980, Quantitative seismology: Freeman and Co.

Anselmetti, F. S., and G. P. Eberli, 1999, The velocity deviation log: A tool to predict pore type and permeability

trends in carbonate drill holes from sonic and porosity or density logs: AAPG 83, 450–466.
Anselmetti, F. S., and G. P. Eberli, 2001, Sonic velocity in carbonates — A combined product of depositional lithology and diagenetic alterations, *in* R. N. Ginsburg, ed., Subsurface geology of prograding carbonate margin, Great Bahama Bank: Results of Great Bahamas Drilling project: SEPM Special Publication 70, 193–216.
Avseth, P. A., T. Mukerji, and G. Mavko, 2005, Quantitative seismic interpretation: Applying rock physics tool to reduce interpretation risk: Cambridge University Press.
Berge, P. A., G. J. Fryer, and R. H. Wilkens, 1992, Velocity-porosity relationships in the upper oceanic crust: Theoretical considerations: Journal of Geophysical Research, **97**, 15239–15254, doi: 10.1029/92JB01464.
Cambois, G., 2000, Can P-wave AVO be quantitative?: The Leading Edge, **19**, 1246–1251, doi: 10.1190/1.1438516.
Castagna, J. P., M. L. Batzle, and R. L. Eastwood, 1985, Relationships between compressional-wave and shear-wave velocities in clastic silicate rocks: Geophysics, **50**, 571–581, doi: 10.1190/1.1441933.
Connolly, P., 1999, Elastic impedance: The Leading Edge, **18**, 438–452, doi: 10.1190/1.1438307.
Ehrenberg, S. N., E. B. Nielsen, T. R. Svånå, and L. Stemmerik, 1998a, Depositional evolution of the Finnmark carbonate platform, Barents Sea: Results from well 7128/6-1 and 7128/4-1: Norwegian Journal of Geology, **78**, 185–224.
Ehrenberg, S. N., E. B. Nielsen, T. R. Svånå, and L. Stemmerik, 1998b, Diagenesis and reservoir quality of the Finnmark carbonate platform, Barents Sea: Results from wells 7128/6-1 and 7128/4-1: Norwegian Journal of Geology, **78**, 225–252.
Fatti, J. L., P. J. Vil, G. C. Smith, P. J. Strauss, and P. R. Levitt, 1994, Detection of gas in sandstone reservoirs using AVO analysis: A 3-D seismic case history using the geostack technique: Geophysics, **59**, 1362–1376, doi: 10.1190/1.1443695.
Goodway, B., T. Chen, and J. Downton, 1997, Improved AVO fluid detection and lithology discrimination using Lamé petrophysical parameters; "λ," "μ," & "λ/μ" fluid stack, from P and S inversions: 67th Annual International Meeting, SEG, Expanded Abstracts, 183–186, doi: 10.1190/1.1885795.
Koefoed, O., 1962, Reflection and transmission coefficients for plane longitudinal incident waves: Geophysical Prospecting, **10**, 304–351, doi: 10.1111/j.1365-2478.1962.tb02016.x.
Li, Y. Y., and J. Downton, 2000, The applications of amplitude versus offset in carbonate reservoirs: Re-examining the potential: 70th Annual International Meeting, SEG, Expanded Abstracts, 166–169, doi: 10.1190/1.1815738.
Ostrander, W. J., 1984, Plane-wave reflection coefficients for gas sands at nonnormal angles of incidence: Geophysics, **49**, 1637–1648, doi: 10.1190/1.1441571.
Rafavich, F., C. H. S. Kendall, and T. P. Todd, 1984, The relationship between acoustic properties and the petrographic character of carbonate rocks: Geophysics, **49**, 1622–1634, doi: 10.1190/1.1441570.
Saberi, M. R., 2010, An integrated approach for seismic characterization of carbonates: Ph.D. dissertation, University of Bergen.
Shuey, R. T., 1985, A simplification of the Zoeppritz equation: Geophysics, **50**, 609–614, doi: 10.1190/1.1441936.
Smith, G. C., and P. M. Gidlow, 1987, Weighted stacking for rock property estimation and detection of gas: Geophysical Prospecting, **35**, 993–1014, doi: 10.1111/j.1365-2478.1987.tb00856.x.
Smith, G. C., and R. A. Sutherland, 1996, The fluid factor as an AVO indicator: Geophysics, **61**, 1425–1428, doi: 10.1190/1.1444067.
Wang, Z., 1997, Seismic properties of carbonate rocks, *in* I. Palaz and K. J. Marfurt, eds., Carbonate seismology: Geophysical developments: SEG 6, 29–52.
Wiggins, R., G. S. Kenny, and C. D. Mcclure, 1983, A method for determining and displaying the shear-velocity reflectivities of a geologic formation: European Patent Application 0113944.
Zoeppritz, K., 1919, On reflection and propagation of seismic waves: Gottinger Nachrichten, **1**, 66–84.

Biographies and photographs of the authors are not available.